Coastal Clouds at the Eastern Margin of the Southeast Pacific: Climatology and Trends

RICARDO C. MUÑOZ

Department of Geophysics, University of Chile, Santiago, Chile

JUAN QUINTANA

Dirección Meteorológica de Chile, Santiago, Chile

MARK J. FALVEY

Department of Geophysics, University of Chile, Santiago, Chile

JOSÉ A. RUTLLANT

Center for Advanced Studies in Arid Zones (CEAZA), La Serena, and Department of Geophysics, University of Chile, Santiago, Chile

RENÉ GARREAUD

Department of Geophysics, and Center for Climate and Resilience Research, University of Chile, Santiago, Chile

(Manuscript received 24 October 2015, in final form 19 March 2016)

ABSTRACT

The climatology and recent trends of low-level coastal clouds at three sites along the northern Chilean coast (18.3°–23.4°S) are documented based upon up to 45 years of hourly observations of cloud type, coverage, and heights. Consistent with the subtropical location, cloud types are dominated by stratocumuli having greatest coverage (>7 oktas) and smaller heights (600–750 m) during the nighttime of austral winter and spring. Meridionally, nighttime cloud fraction and cloud-base heights increase from south to north. Long-term trends in mean cloud cover are observed at all sites albeit with a seasonal modulation, with increasing (decreasing) coverage in the spring (fall). Consistent trend patterns are also observed in independent sunshine hour measurements at the same sites. Cloud heights show negative trends of about 100 m decade^{-1} (1995–2010), although the onset time of this tendency differs between sites. The positive cloud fraction trends during the cloudy season reported here disagree with previous studies, with discrepancies attributed to differences in datasets used or to methodological differences in data analysis. The cloud-base height tendency, together with a less rapid lowering of the subsidence inversion base height, suggests a deepening of the coastal cloud layer. While consistent with the tendency toward greater low-level cloud cover and the known cooling of the marine boundary layer in this region, these tendencies are at odds with a drying trend of the near-surface air documented here as well. Assessing whether this intriguing result is caused by physical factors or by limitations of the data demands more detailed observations, some of which are currently under way.

1. Introduction

The coast of northern Chile (19–24°S, ~70°W) lies at the boundary between two remarkably contrasting climatic environments. To the east, the extremely arid Atacama Desert and the high Andes Cordillera (>4000 m MSL) are located no farther than 300 km from the coast. To the west, the subsidence associated with the semipermanent southeast (SE) Pacific anticyclone and the cold SE Pacific waters combine to produce a cool and humid marine boundary layer frequently capped by a stratocumulus (Sc) layer. The large extension and the persistence of this Sc layer make it an important factor in the global energy budget, acting as a cooling agent

Corresponding author address: Ricardo C. Muñoz, Dept. of Geophysics, University of Chile, Av. Blanco Encalada 2002, Santiago, Chile. E-mail: rmunoz@dgf.uchile.cl

DOI: 10.1175/JCLI-D-15-0757.1

because of its effect on Earth's mean albedo (Klein and Hartmann 1993; Bretherton et al. 2004). As such, the SE Pacific Sc cloud layer has been the subject of several observational and modeling studies aiming at improving the understanding of its dynamics and the representation of these clouds in climate models (Mechoso et al. 2014).

While closely related to the Sc clouds existing offshore, the low-level clouds along the northern Chilean coast are also influenced by local circulations induced by the land–sea contrast and prominent coastal topography. As a result, coastal clouds in this region show a marked diurnal, synoptic, and seasonal variability, whose description is of importance for several applications including surface and air transportation, solar energy resources, and tourism.

Several previous works have addressed climatological features and tendencies of meteorological variables measured at the coast of northern Chile. Muñoz et al. (2011) presented a 29-yr climatology of surface meteorology and vertical temperature and wind structure at Antofagasta (23.4°S, 70.4°W). In particular, they described the differences observed in this coastal boundary layer depending on the presence of low-level clouds. The current work can be considered a complement to Muñoz et al. (2011) aimed at documenting in more detail the climatology and trends of coastal clouds in this region. Schulz et al. (2012) described the interannual and long-term tendencies in precipitation, subsidence inversion height, and cloudiness along the arid coast of northern Chile. Of special relevance to this work, they reported a strong decrease in total cloudiness since the 1970s affecting the northernmost portion of the Chilean coast. Falvey and Garreaud (2009) and Vuille et al. (2015), on the other hand, documented a cooling trend in near-surface temperatures in the coastal region of the SE Pacific over the last decades, at least partially explained by the cold phase of the Pacific decadal oscillation (PDO) that has prevailed since the late 1980s (Trenberth and Fasullo 2013). Above the boundary layer, however, they report a warming trend in the free troposphere suggestive of a strengthening of the downward branch of the Hadley cell over the study region. In terms of climatological analyses of cloud observations for this region, Quintana and Berríos (2007) and Berríos (2008) provided a preliminary description of the variability of coastal clouds along northern Chile, while at a global scale, Eastman and Warren (2013, 2014) compiled and documented a cloud climatology based on surface observations, including the three stations analyzed herein. Finally, in a recent work Seethala et al. (2015) analyzed corrected satellite observations of low-cloud fractions to document decadal trends (1984–2009) of cloudiness over several subtropical regions. For the region off the west coast of South America, they show a broad and significant increase in annual mean low-cloud amount. By examining the attendant trends of meteorological variables from reanalysis products, they attribute this increase in low-level clouds mostly to an increment in the estimated inversion strength capping the marine boundary layer, aided by cooler sea surface temperatures and enhanced cold air advection.

The present work aims at providing a more comprehensive description of the climatology and trends of coastal clouds in this region by using a more detailed and extended database than those of previous studies. Section 2 of the paper describes the region of interest and the databases used. The climatological features of low-level coastal cloud fractions and heights at the three sites are presented in section 3, together with their recent trends. Section 4 does the same for meteorological variables such as temperature, humidity, and sunshine hours, in an effort to verify the consistency between the documented variability of clouds and those of closely related variables. This consistency is discussed in section 5 as well as some disagreements that we find between our results and those of previous works. Section 6 summarizes our findings and describes some questions left open by them.

2. Sites and data

The main dataset analyzed in this study corresponds to hourly cloud observations at the three major airports along the northern Chilean coast: Arica (WMO station 85406; 18.33°S, 70.33°W; 58 m MSL), Iquique (WMO station 85418; 20.53°S, 70.18°W; 52 m MSL), and Antofagasta (WMO station 85442; 23.43°S, 70.43°W; 135 m MSL). Figure 1 shows the location of these sites together with a topographic map and an example of a typical morning cloud field over the region. The period of analysis extends from 1969 to 2013 at Arica and Antofagasta (45 years) and from 1981 to 2013 at Iquique (33 years), as before 1981 the Iquique airport operated in a different location. While data prior to 1969 exist at Arica and Antofagasta, these are available only at 3-hourly intervals and with reduced nocturnal coverage. In fact, regular hourly cloud observations at Arica between 0100 and 0800 UTC only begin in April 1972.

Cloud observations are performed by professional observers from the Chilean National Weather Service supporting aeronautical operations at these airports. During daytime, they use local topographic references to estimate cloud-base heights. At night, heights are estimated by using a ceiling light projector located at a known distance from the observing point and a clinometer that measures the elevation angle to the point marked by the light reaching the cloud base.

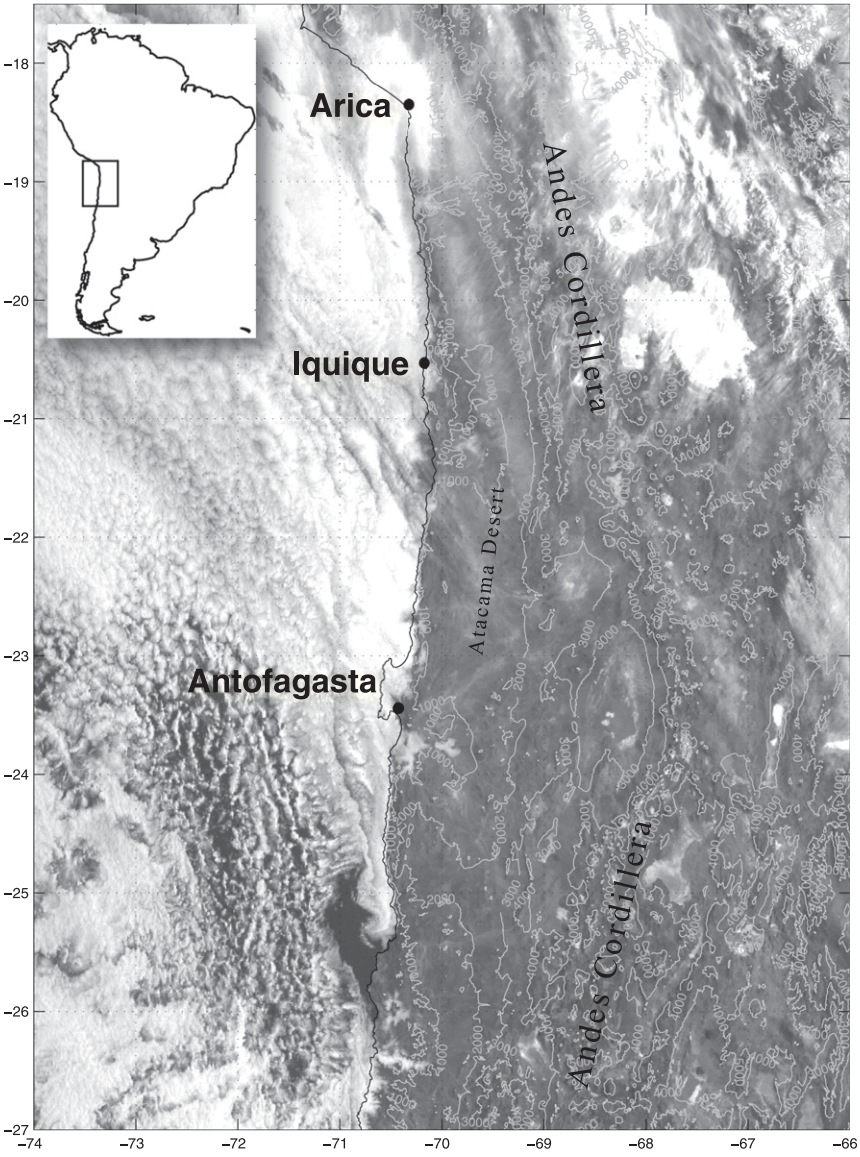

FIG. 1. Regional topography and location of three sites. Contours drawn from 1000 to 5000 m MSL every 1000 m. Rectangle in the inset shows location of the study region in South America. The regional cloud field is illustrated by a GOES visible image for 1145 UTC 27 September 2014.

Since June 2006 this system was aided by a laser ceilometer at Arica, although no change in the data is apparent. Some previous studies on cloud climatologies warn about the difficulties of cloud observations at night (Hahn et al. 1995) and even avoid using them (Eastman and Warren 2013). We argue that in this particular region nighttime appreciation of low clouds is not especially hard for a trained observer because the free troposphere above the marine boundary layer is extremely clear and dry, as attested by the presence of several astronomical observatories located in the coastal mountains above the marine boundary layer (Garreaud 2011; Rondanelli et al. 2015). Thus, even in the absence of lunar illumination, low-level clouds can be well contrasted against the dark black starred sky background provided by the dry and clear free troposphere.

The basic dataset analyzed here consists of hourly reports of up to four cloud layers, with documentation of cloud type, cloud fraction, and cloud-base height. These data correspond to the cloud descriptors included in group 8 of section 3 of the synoptic (SYNOP) message (WMO 1995) and similar data gathered in the preparation of METAR messages. The cloud fraction refers to the fraction of sky occupied by clouds in each layer and is measured in oktas (1 okta ≡ 1/8 of total sky cover). Figure 2 shows the basic statistical characterization of these data, including the distributions of the number of

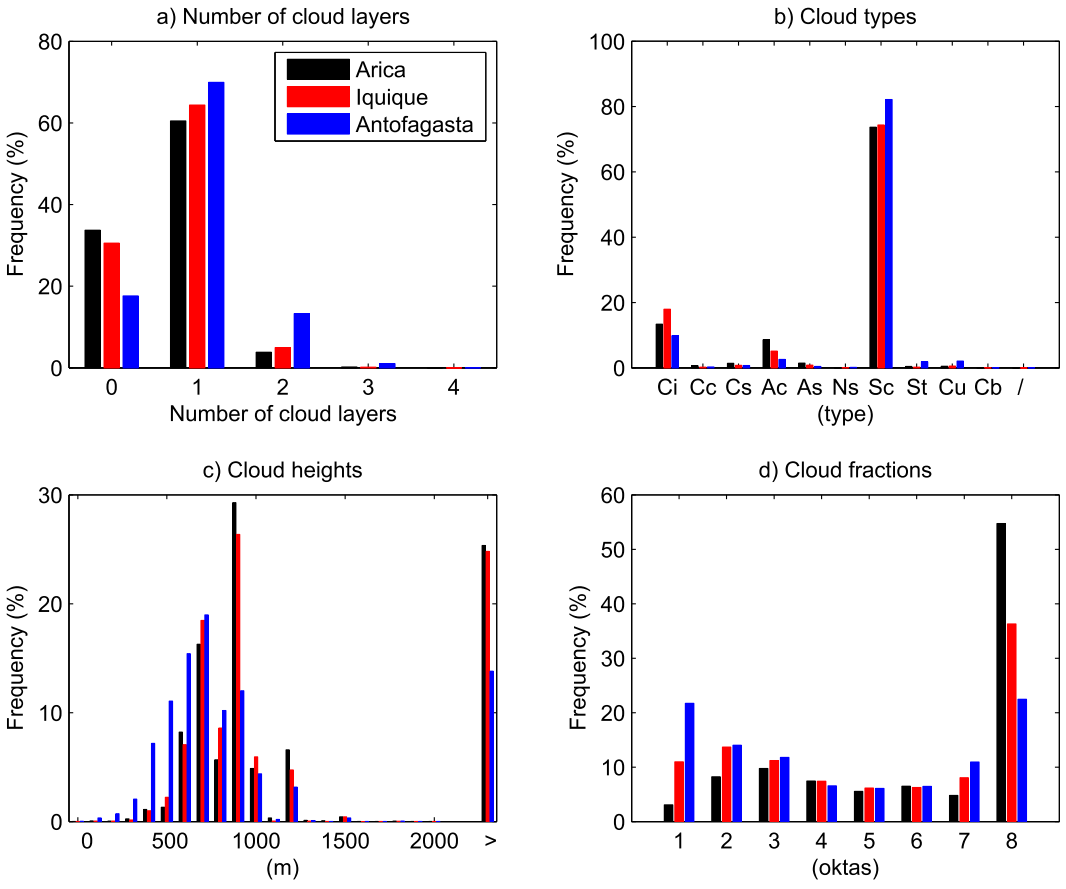

FIG. 2. Statistical characterization of basic hourly cloud datasets at Arica (1969–2013), Iquique (1981–2013), and Antofagasta (1969–2013). (a) Histograms of number of cloud layers reported each hour. (b) Histograms of cloud types reported. (c) Histograms of cloud-base heights reported. Bars at the right combine all clouds with heights larger than 2000 m. (d) Histograms of cloud fractions reported.

cloud layers reported (Fig. 2a), cloud types (Fig. 2b), cloud heights (Fig. 2c), and cloud fractions (Fig. 2d). Consistent with their geographic location, the observed cloud types at the three sites are dominated by Sc with heights below 1500 m and typically large sky coverage fraction. It must be pointed out that the cloud height distributions in Fig. 2c are not smooth but show several local maxima below 1500 m related to standard cloud-base heights used in aeronautical practice.

Variables representative of low clouds are constructed based on the basic cloud data. First, cloud types of stratocumulus, stratus, or cumulus and cloud heights below 2000 m are selected. In cases that more than one layer of such clouds is reported, the layer with higher cloud fraction (usually the highest) is chosen as representative of the low clouds for this hour. In this way we construct hourly series of cloud height and cloud fraction of low-level clouds for the three sites.

Ancillary measurements used to provide context to the cloud data analysis include surface observations of temperature and dewpoint, sunshine hours, and routine 1200 UTC (0800 LT) radiosondes performed daily at Antofagasta airport. The temperature and dewpoint database is constructed by blending data from the Chilean National Weather Service (DMC) with NOAA's integrated surface hourly dataset (ISD). The former has a longer record and generally better quality, although it contains some anomalous peaks probably due to errors when digitizing the original paper records. The latter has hourly data since 1973 (at Arica and Antofagasta) and has been used here in order to filter and correct the DMC dataset. Thus, the temperature and dewpoint database used in the current analysis contains hourly data from 1973 to 2013 for Arica and Antofagasta and from 1981 to 2013 for Iquique. From 2006 to 2010 the dewpoint data at Arica and Iquique has only 3-hourly reports, which were filled by simple interpolation in time in order to homogenize the temporal resolution of the datasets.

Sunshine hours are recorded by Campbell–Stokes heliographs at the three sites. Every day a sensitive

band is put in these instruments, which is marked by a burnt trace when direct solar radiation impinges upon the instrument. The daily bands are subsequently read by the observer, who estimates and reports the hourly fractions of direct sunshine received [sunshine hour fraction (SH)] as well as the total sunshine hours for each day. The SH data analyzed here is for the period 1977–2013 at Arica and Antofagasta and 1981–2013 for Iquique. Data before 1977 at Arica and Antofagasta are not considered because their variability appears different than that for the subsequent period and further detailed analysis would be required to assess whether the change is real or artificial.

Finally, vertical profiles of temperature and humidity are characterized by means of the routine 1200 UTC (0800 LT) radiosondes launched at Antofagasta airport. We use the database compiled and described by Muñoz et al. (2011), starting in 1979 and updated until 2013. Temperature profiles are used also to determine a subsidence inversion base height (ZI), as explained in the same reference.

3. Climatology and trends of cloud data

Figure 3 shows the diurnal and annual cycles of low-cloud fractions (CFs) and cloud-base heights (CHs). At the three sites the mean CF is greatest during nighttime hours in the months from July to September (austral late winter–early spring). The mean CF decreases during the austral summer with lowest overall values in February. CF also decreases sharply after sunrise, reaching minimum values in the afternoon (1500–2100 UTC). The diurnal and annual cycles of CH follow closely those of CF, although with opposite phase, clouds being lower during winter nighttime hours and higher during the daytime and during summer. The diurnal cycles of CF and CH at these coastal sites appear quite similar to those commonly reported for marine stratocumulus (Wood 2012).

Comparison of CF patterns at the three sites in Fig. 3 suggests that CF increases to the north, with Arica showing mean CF values above 7 oktas during most of nighttime hours in the winter period. At this station the morning dissipation of low clouds appears to occur about 2–3 h later than in Iquique and Antofagasta, a feature that is confirmed by sunshine records described in section 4a. The climatology of CH, on the other hand, is similar at Arica and Iquique (750–1050 m), while significantly lower heights are reported at Antofagasta (600–850 m).

Time series of annual mean CF and CH are shown in Fig. 4. Shaded regions in Figs. 4a,b represent 95% confidence intervals for the annual mean values. The intervals were calculated for each year using a 1000-sample Monte Carlo simulation assuming normally distributed random observational uncertainties of 1 okta for cloud fraction and 200 m for cloud height in their daily averages (Williams et al. 2015). Bootstrap resampling was used to take into account intraannual variability (Wilks 2005, 166–170). None of the CF series show a clear tendency, and the correlation between the annual averages is modest (largest correlation coefficients of $r = 0.64$ found for Arica–Iquique and Iquique–Antofagasta pairs). The series of CH, in contrast, show marked decreasing trends, although the period in which they are most noticeable is different for each site. Mean CH values at Antofagasta, for example, decreased by about 200 m from 1985 to 2005, being relatively constant afterward. At Iquique the decreasing trend begins around 1990 while at Arica it appears between 1995 and 2000. The consistency of these trends in CH with those of other variables is discussed in section 5. For a similar climatological setting as that of our study region but in the west coast of North America, Williams et al. (2015) have recently reported lowering of cloud bases and increased cloud frequencies for islands off the coast of Southern California. At the coast itself, they report the opposite trends and attribute them to urbanization effects.

Figure 5 shows the diurnal and monthly variation of CF and CH tendencies. The statistical significance of the trends was determined using a two-tailed hypothesis test at the 5% level, where trend probabilities were determined from a 1000-member synthetic null distribution derived by randomly reordering the annual series. In the case of CH, the tendencies were restricted to the 1995–2010 period, in which all three stations show consistent lowering of cloud bases (see Fig. 4b). The small tendencies observed in the annual CF averages in Fig. 4a actually disguise the presence of opposing seasonal trends (Fig. 5, left). In winter and spring (June–December) there is an apparent increasing trend of CF at all sites, while the opposite occurs in summer and fall (January–May). Moreover, a latitudinal gradient is perceived, with stronger positive trends in CF at Antofagasta and stronger negative trends at Arica. The positive tendency in CF during winter and spring nights at this latter station appears to contradict the strongly negative trends in cloud fraction reported for Arica by Schulz et al. (2012), a matter that will be discussed in section 5. The tendencies of CH, on the other hand, show a seasonal structure only in the two more northern stations, although the positive summer trends at these stations have little statistical significance. The general pattern of CH trends is thus dominated by the marked negative trend already shown in Fig. 4.

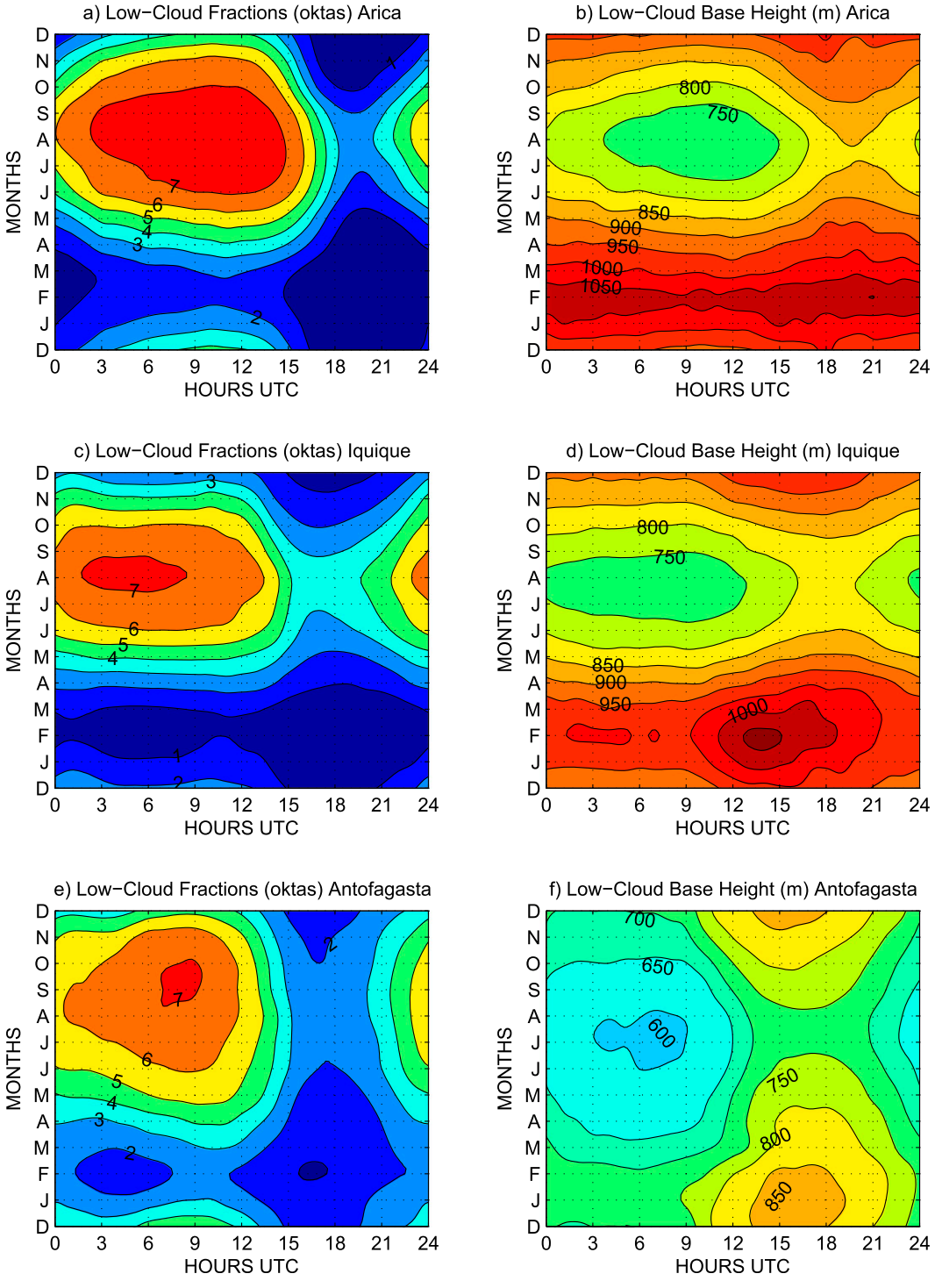

FIG. 3. Diurnal and annual mean cycles of low-cloud (left) fractions and (right) base heights for (a),(b) Arica, (c),(d) Iquique, and (e),(f) Antofagasta. Period considered in the climatology is 1969–2013 at Arica and Antofagasta, and 1981–2013 at Iquique (LT = UTC − 4 h).

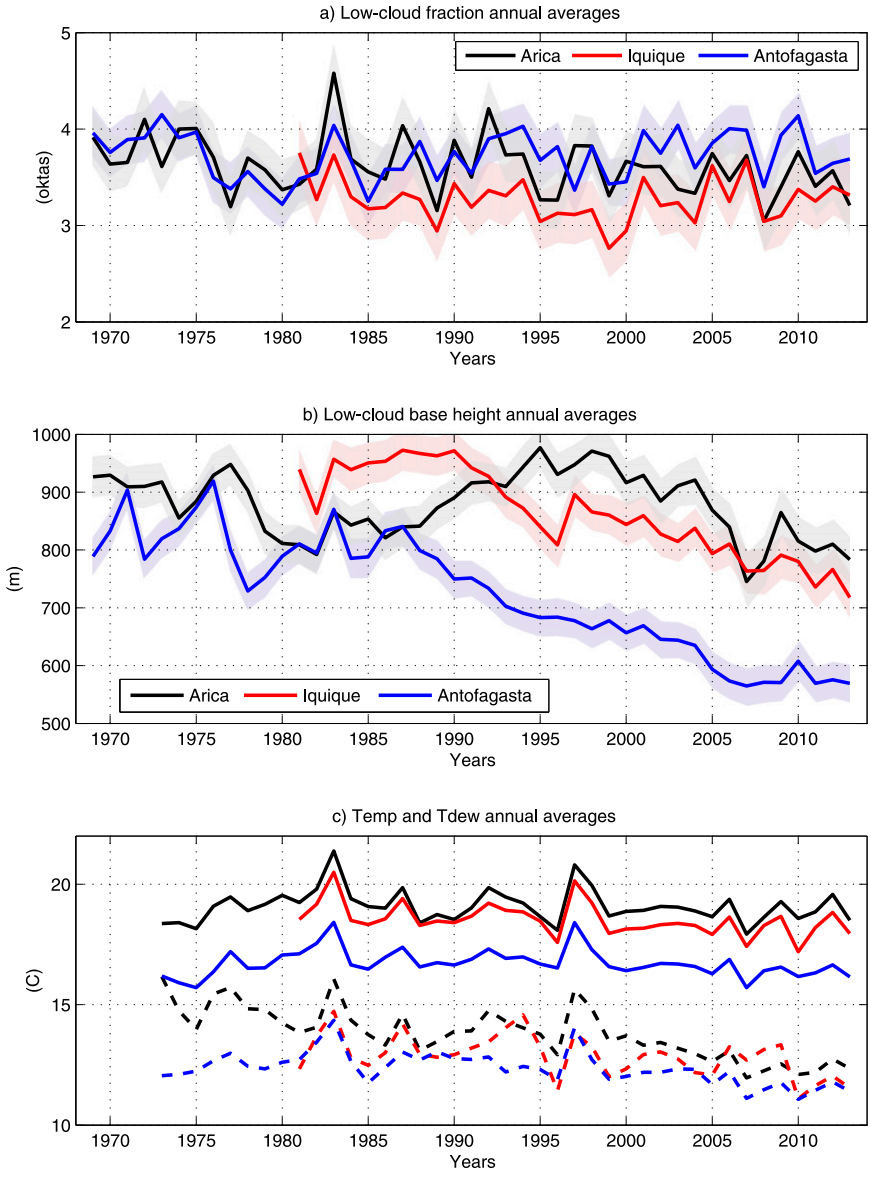

FIG. 4. Series of annual averages of (a) low-cloud fractions, (b) cloud-base heights, and (c) temperature (solid) and dewpoint temperature (dashed) for Arica (black), Iquique (red) and Antofagasta (blue) stations. Shading in (a) and (b) shows estimated 95% confidence intervals for annual averages.

The annual averages shown in Fig. 4 lack a clear mark of ENSO variability. Only the 1982/83 El Niño event is partly reflected by a larger CF in Fig. 4a, but subsequent events are not as clear. A clearer depiction of the ENSO effect on CF is obtained by plotting the time series of 3-month averages of CF (not shown). In this case, conspicuous peaks of CF are obtained at Arica station for El Niño events of 1983, 1992, and 1997/98. Less marked peaks are observed at the other more southern stations. The ENSO effect on CH, on the other hand, is much weaker. The larger interannual variability of CH observed in years prior to 1985 may be due to the more discretized values used in the reports, as mentioned in section 2.

4. Climatology and trends of related variables

a. Sunshine hours

The sunshine hour fractions recorded by the Campbell–Stokes heliographs provide an independent means of characterizing cloud fractions, at least during daytime.

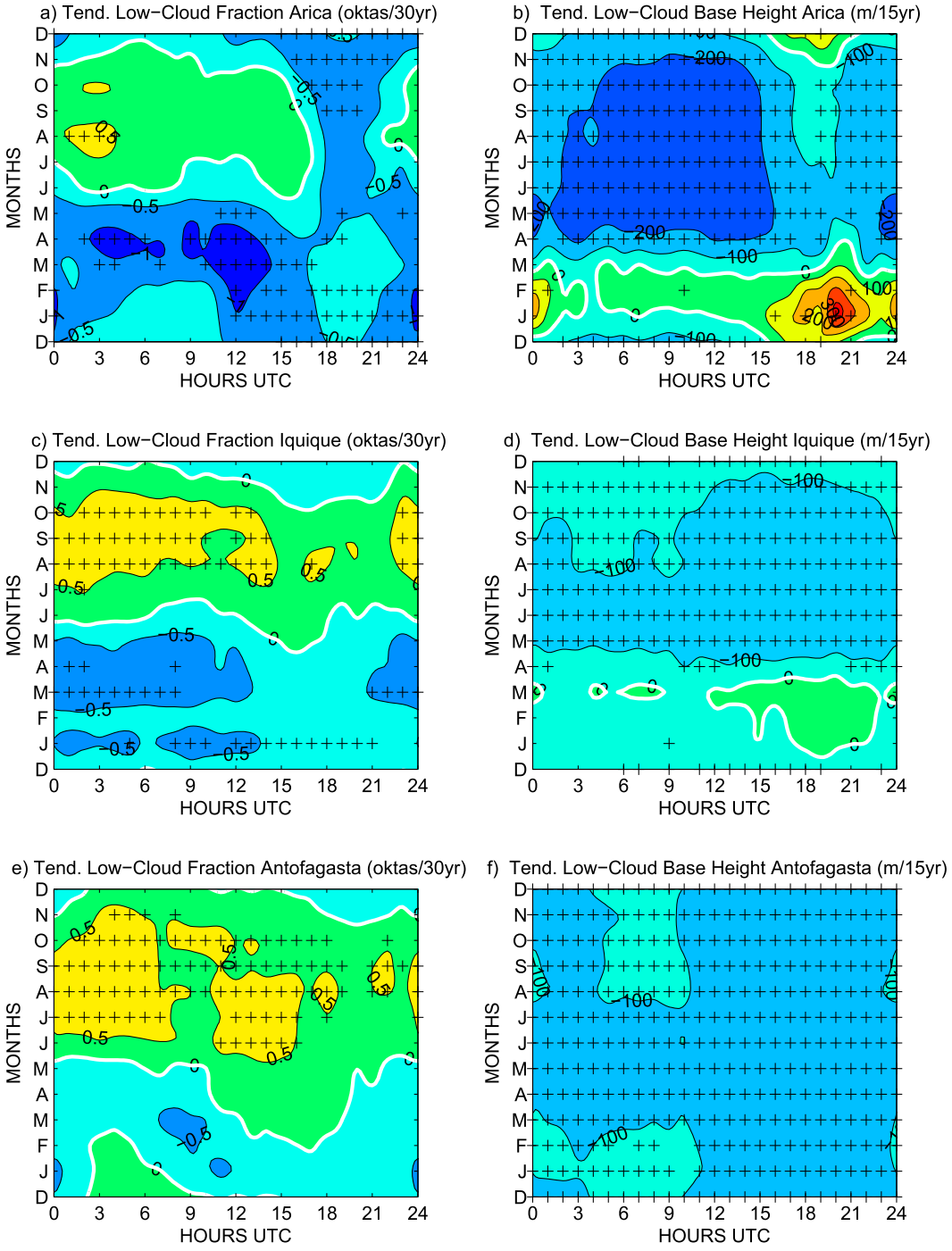

FIG. 5. Diurnal and annual variation of tendencies in (left) CF and (right) CH for (a),(b) Arica, (c),(d) Iquique, and (e),(f) Antofagasta. CF tendencies are computed for period 1981–2013 and CH tendencies are computed for period 1995–2010. A 3-month-averaging smoothing filter has been applied to average values prior to compute the monthly tendencies. Crosses indicate trends with statistical significance at a 5% level.

Figure 6 shows bivariate histograms of CF and sunshine hours at the three sites. There is a very good agreement between both datasets, especially considering the fact that the heliographs provide a measure of the time fraction of cloud cover within each hourly interval whereas the CF measurements are essentially instantaneous estimations of the spatial fraction of cloud cover at each observation time. At Arica, and to a lesser

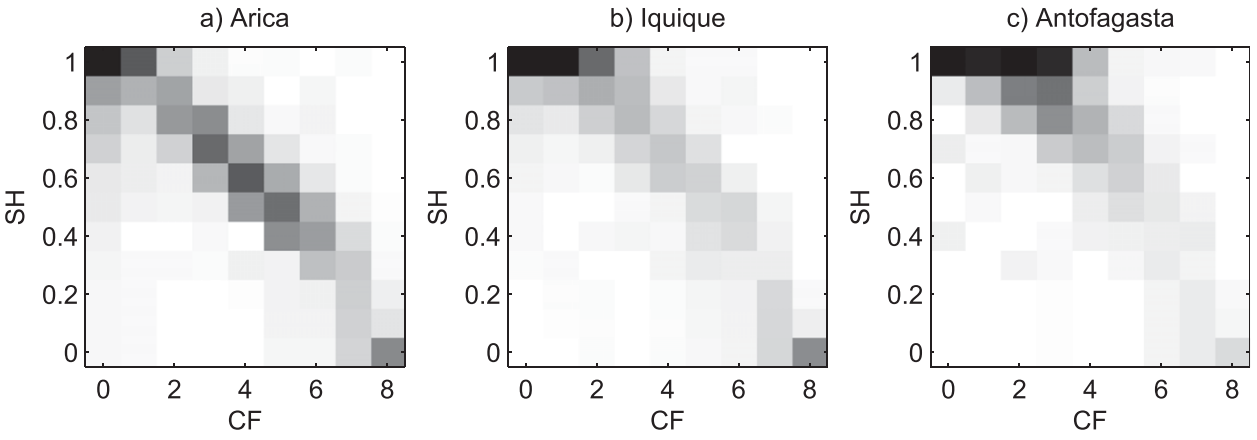

FIG. 6. Bivariate histograms of SH and CF for (a) Arica, (b) Iquique, and (c) Antofagasta. Values correspond to averages between 1000 and 1500 LT. Gray shading is proportional to the number of cases in the bivariate histogram for each (CF, SH) class, with full black representing 800 or more class members. Lower-right cells in (a),(b), and (c) correspond to 438, 425, and 132 class members, respectively. Period of analysis is 1977–2013 for Arica and Antofagasta and 1981–2013 for Iquique.

extent at Iquique, there is a relatively large fraction of cases in which low CF is accompanied by small sunshine hour fractions. As CF has been restricted to describe low-level clouds, these cases are explained by the presence of middle and high clouds that reduce the direct solar radiation reaching the surface but are not included in the CF index.

The mean diurnal cycles of SH at the three sites are presented in Fig. 7a. As a reference, we added into the figure the theoretical mean hour fraction in which the sun is above the horizon. The most salient feature in these diurnal cycles is the reduced SH at Arica during the morning hours, which confirms the later-dissipating clouds at this site described in the analysis of Fig. 3. Note that the presence of coastal topography and the Andes to the east of all sites may reduce measured sunshine hours during the early morning.

The seasonal cycle of SH is depicted in Fig. 7b. SH varies throughout the year for two main reasons: the seasonal changes in the number of hours during which the sun is above the horizon and the presence of clouds. To concentrate on the cloud factor, we plot in Fig. 7b an SH deficit, computed as the difference between the maximum daylight duration and the actual observed SH. This deficit should be more clearly related to the CF at each site. Indeed, the deficit maximizes around August at Arica and Iquique and around September–October at Antofagasta, which is generally consistent with the seasonal distribution of CF in Fig. 3. The SH deficit reaches a minimum around February–March, again in agreement with CF observations. In terms of latitudinal variation, Fig. 7b suggests that during winter and early spring the cloud effect increases from south to north, which is also consistent with the CF patterns in Fig. 3.

Finally, in terms of SH trends, Fig. 8 illustrates their seasonal variation. Although with reduced statistical significance, SH trends at the three sites show a seasonal pattern consistent with the trends in CF: SH appears to be decreasing from June to October (associated with increases in CF observed in Fig. 5) and increasing during summer and fall (associated with negative CF trends in Fig. 5). The general consistency between the climatology and trends of SH with the corresponding variations of CF can be considered to provide support to both datasets.

b. *Surface temperature and dewpoint*

Figure 9 shows the mean diurnal and annual cycles of surface temperature, dewpoint, and dewpoint depression at the three sites. Dewpoint is closely related to absolute humidity, while dewpoint depression relates more to the relative humidity of the surface air. The temperature shows diurnal and seasonal variations with mean amplitudes within 3°–5° and 5°–7°C, respectively. The rather modest diurnal amplitudes are likely associated with the coastal location of these stations. A northerly increase in mean temperatures is observed as well, consistent with what can be expected for this geographic region. In terms of humidity, the dewpoint in the center panels of Fig. 9 shows little diurnal variation and a seasonal amplitude of about 5°C, with maximum values in the summer and minimum values in winter. The close phase match between the seasonal variation in temperature and dewpoint produces very little seasonal change in the mean nocturnal dewpoint depression (Fig. 9, right), pointing to fairly constant nocturnal relative humidity throughout the year. The daytime temperature increases, however, make the

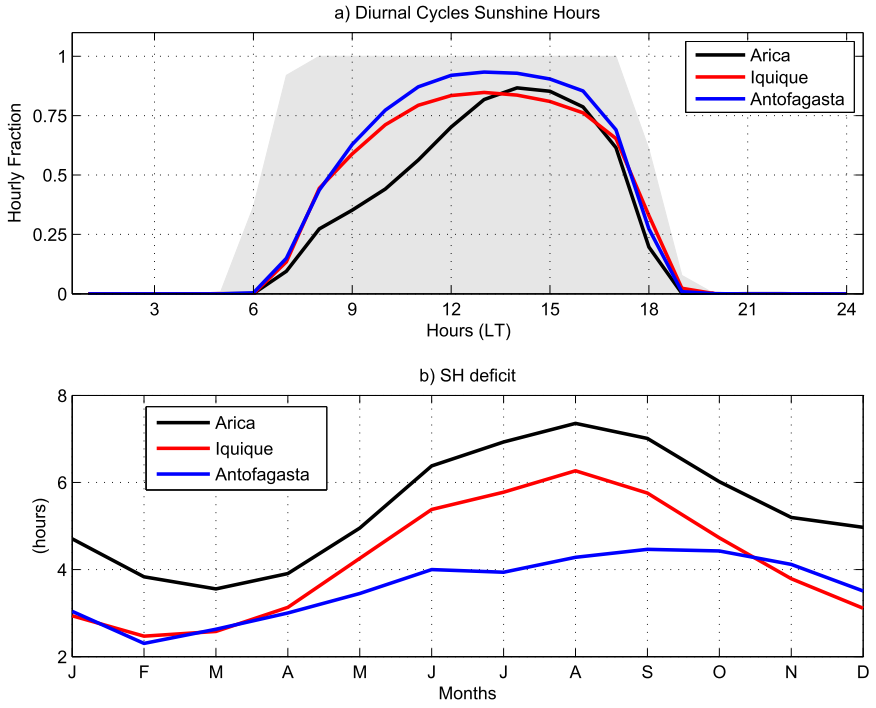

FIG. 7. (a) Diurnal cycles of sunshine hours at Arica (black), Iquique (red) and Antofagasta (blue). Shading indicates theoretical hourly fraction of the sun above the horizon (averaged for the three stations, individual cases being very similar). (b) Monthly variation of the daily sunshine hour deficit for the three stations. Deficit is computed as a difference of the theoretical sun-above-the-horizon fraction and the actual sunshine hours summed over the full day. Period of analysis is 1977–2013 for Arica and Antofagasta and 1981–2013 for Iquique.

dewpoint depression increase during the day, especially in the summer.

The series of annual averages of temperatures and dewpoints have been shown in Fig. 4c. The strong hallmark of the El Niño events of 1982/83 and 1997/98 is clearly seen in the temperature records of the three sites. They are also seen in the dewpoints, therefore having little effect on the dewpoint depression. The temperatures show a weak cooling tendency at all sites, a feature already described and discussed by Falvey and Garreaud (2009) and Vuille et al. (2015). Whether or not this temperature trend can be attributed to an increasing trend in upwelling-favorable winds is not a settled point. While Sydeman et al. (2014) claim a strengthening in the upwelling-favorable winds in the broad Humboldt system, Varela et al.'s (2015) results based on high-resolution reanalysis suggest for the last decades a weakening of the upwelling in central Chile, south of the Antofagasta region. The dewpoints in Fig. 4c, on the other hand, show an apparently larger decreasing trend as compared to that of temperatures, suggesting a possible drying tendency of the near-surface air at these coastal sites. This result is intriguing and will be discussed further in section 5.

The diurnal and seasonal patterns of the observed trends in temperature, dewpoint, and dewpoint depression are shown in Fig. 10. Statistical significance of these trends was assessed with the same methodology as that described for cloud fraction and cloud heights. The temperature cooling tendencies have a strong diurnal modulation, with larger magnitudes in daytime and smaller values during the night, especially at Arica and Iquique. This behavior was already described by Falvey and Garreaud (2009), who found larger cooling trends of maximum temperatures compared to smaller and even positive trends of minimum temperatures at Arica. Their interpretation of this effect was that the coastal sea breeze circulation more efficiently transports the oceanic cooling into the coastal stations during daytime as compared to nighttime. The stronger cooling trend in dewpoint (Fig. 10, center), on the other hand, does not show a clear diurnal or seasonal pattern at all stations. As a result, the tendencies in dewpoint depression show patterns following those of the temperature: drying during the nights, especially at Arica, and small tendencies or even increasing humidity during daytime (although less significant).

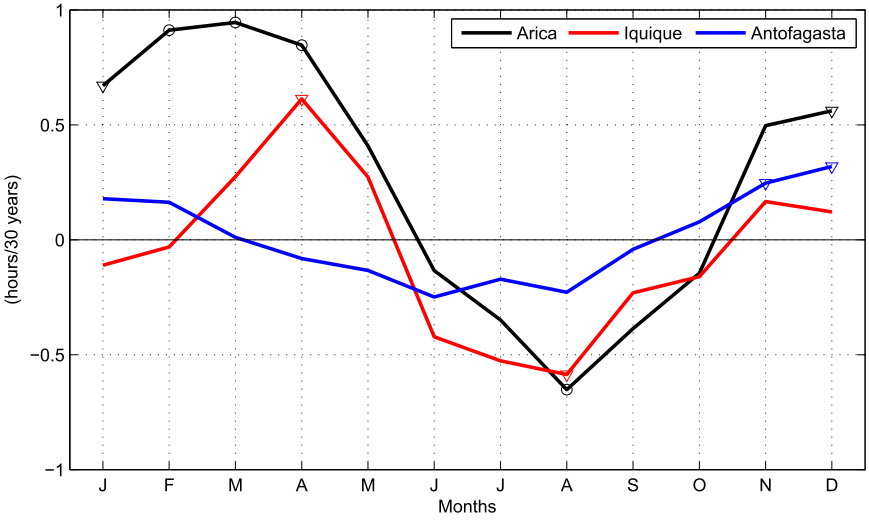

FIG. 8. Seasonal variation of tendencies of sunshine hours at Arica (black), Iquique (red) and Antofagasta (blue) expressed in units of oktas $(30\,\text{yr})^{-1}$. Period of analysis is 1981–2013 for the three sites. A 3-month-averaging smoothing filter has been applied to averages prior to the computation of monthly tendencies. Circles (inverted triangles) mark trends with statistical significance at a 10% (20%) level.

5. Discussion

a. *Comparison of cloud trends reported by previous studies*

1) CLOUD FRACTION TENDENCIES AT ARICA OF SCHULZ ET AL.

The small annual cloud fraction tendencies at Arica in Fig. 4a and the positive spring tendencies in Fig. 5a appear at odds with the strong negative trend in cloudiness documented for this station by Schulz et al. (2012). They report annual cloudiness at Arica changing from about 4.5–5.0 oktas in 1960–70 down to between 3.0 and 3.5 oktas over the period 2000–08 (Schulz et al. 2012, their Fig. 11a). To investigate these conflicting results, we attempted to reproduce their analysis based upon our basic data. Schulz et al.'s (2012) analysis of cloud cover is based on meteorological yearbooks, in which monthly averages of total cloudiness are reported at only three times of day: 1200, 1800, and 2400 UTC. Our basic data, on the other hand, are hourly reports of up to four cloud layers, as described in section 2. The main two differences in the analysis are therefore the use of total versus low-level clouds and the use of three specific hours in the diurnal cycle versus using all available hourly observations.

To obtain a more direct comparison between our results and those of Schulz et al. (2012), we computed a middle and high cloud cover index for clouds with base heights above 2000 m (we refer to them together as high clouds) by applying the same methodology used to create the index of low-cloud fraction. We then computed annual averages using only 1200, 1800, and 2400 UTC for the low and high clouds, as well as for their sum considered to be a total-cloud index. The series of annual means of these indices is shown in Fig. 11. Our total-cloud index compares well with that of Schulz et al. (2012), showing a similar drop between 1980 and 2010. Our dataset, however, allows us to assess the contribution of low- and high-level clouds to the negative trend reported in Schulz et al. (2012). Figure 11 suggests that the total cloud cover decrease at this site is mainly due to less frequently reported mid- and high-level clouds, more than to a drop in low-level clouds. Moreover, the modest decrease in low-level clouds shown in Fig. 11 is mostly due to the three specific hours reported in the annals. As shown in Fig. 3, 1200, 1800, and 2400 UTC do not represent well the hours of low-level clouds, and the tendencies at these hours are biased toward negative values (Fig. 5). As a final comment, the decrease of mid- and high-level clouds shown in Fig. 11 must be taken cautiously as the high prevalence of low-level clouds at this site makes the observations of middle and high clouds less robust, and their cover fraction is most probably underestimated by these observations. On the other hand, a trend in mid- and high-level clouds could in principle affect observations of low-level clouds, especially in the night, but this effect is difficult to assess with the available database.

2) CLOUD TENDENCIES OF EASTMAN AND WARREN

Eastman and Warren (2013, hereafter EW13) updated until 2009 the 1971–96 global database of surface cloud observations described by Warren et al. (2007).

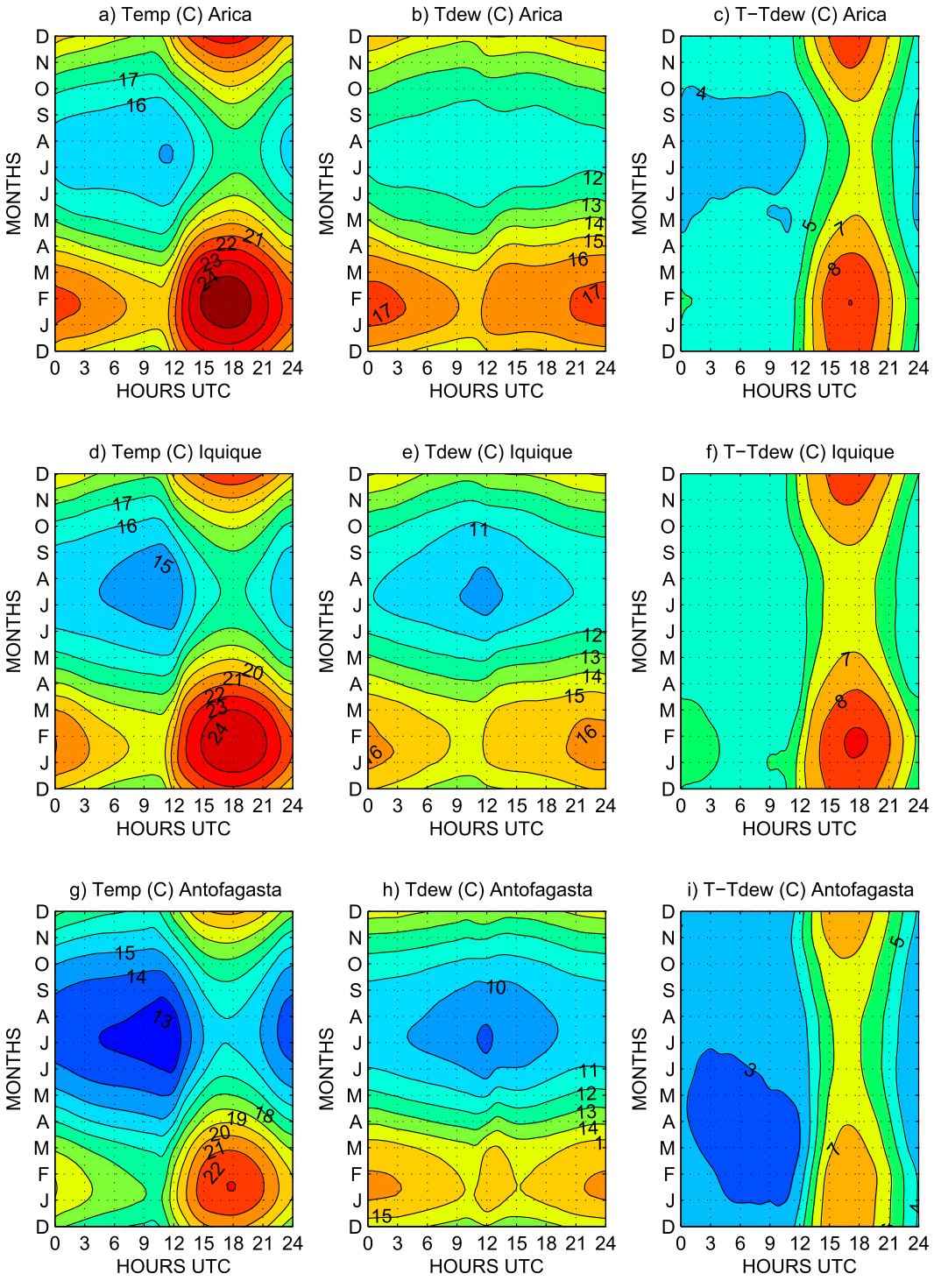

FIG. 9. Diurnal and annual mean cycles of (left) surface temperature, (center) dewpoint temperature, and (right) dewpoint depression for (a)–(c) Arica, (d)–(f) Iquique, and (g)–(i) Antofagasta. Period considered in the climatology is 1973–2013 at Arica and Antofagasta and 1981–2013 at Iquique.

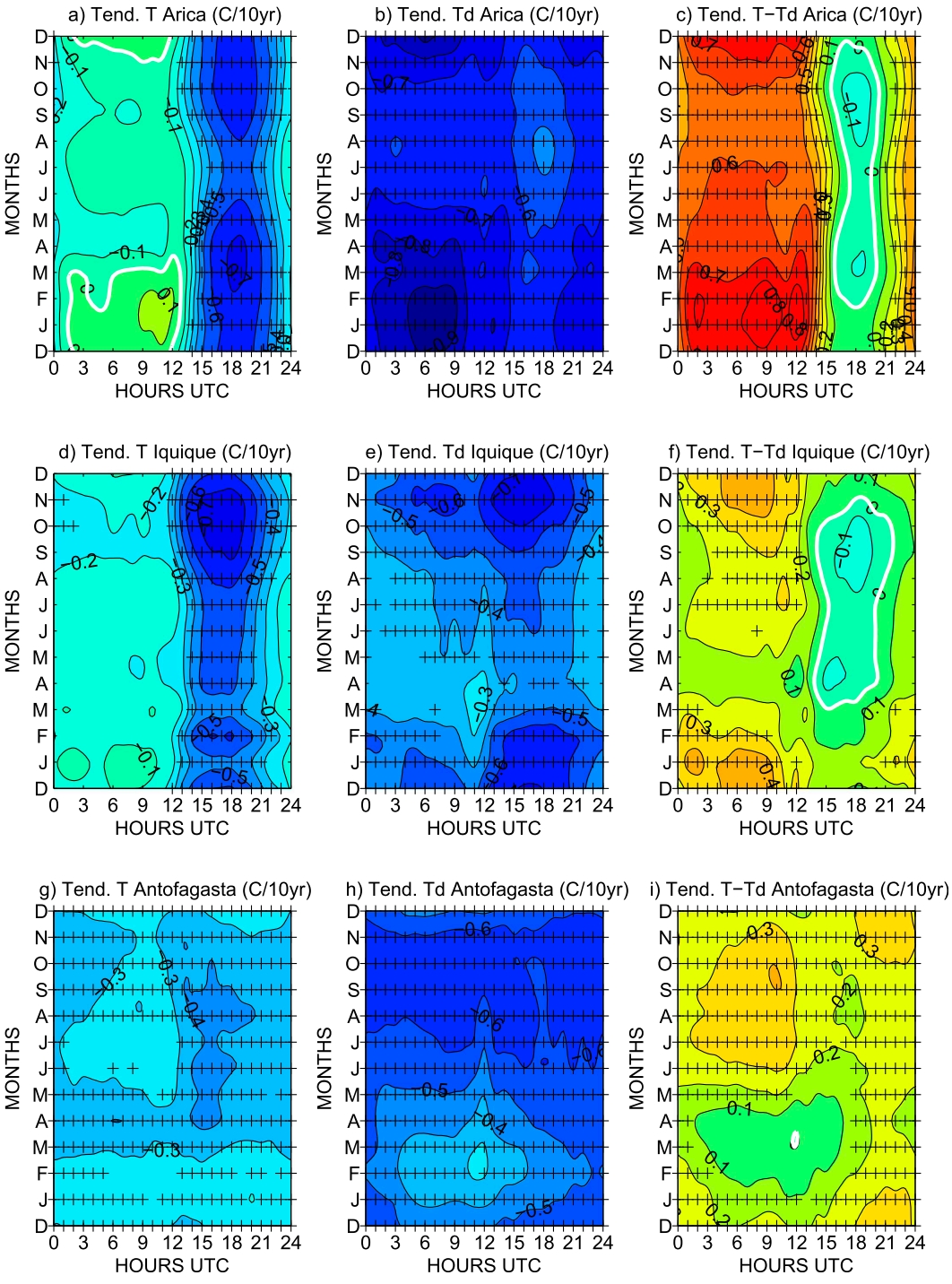

FIG. 10. Diurnal and annual variation of tendencies in (left) surface temperature, (center) dewpoint temperature, and (right) dewpoint depression for (a)–(c) Arica, (d)–(f) Iquique, and (g)–(i) Antofagasta. Period considered in the analysis is 1981–2013 for the three sites. A 3-month-averaging smoothing filter has been applied to average values prior to compute the monthly tendencies. Crosses indicate trends with statistical significance at a 5% level.

For the coastal region of northern Chile EW13 report an average decrease of stratiform clouds of 0.4% decade^{-1} [equivalent to 0.1 okta (30 yr)$^{-1}$]. In their companion website, they provide a more complete characterization of the climatology and trends of this cloud database. Accordingly, the trends of stratiform clouds for this region are +0.3%, −1.4%, 0%, and −0.6% decade^{-1} for the summer, fall, winter, and spring periods, respectively.

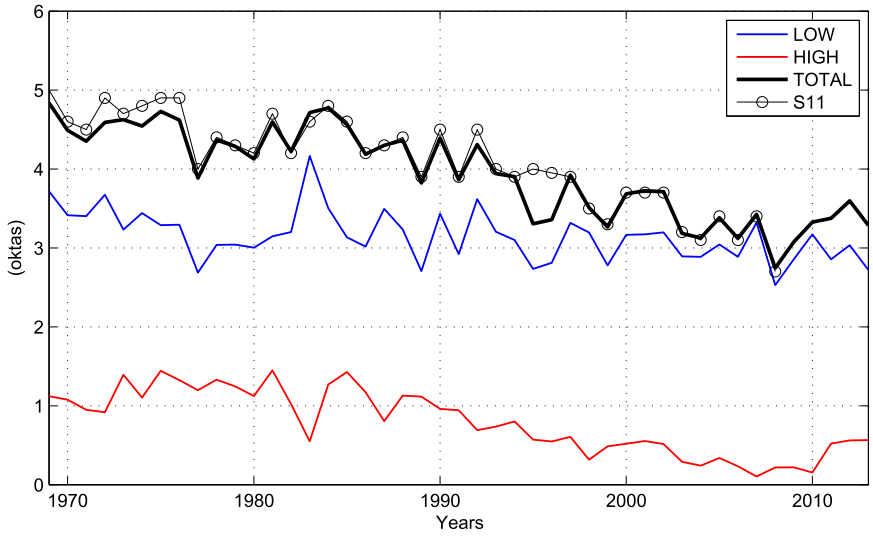

FIG. 11. Annual averages of low-cloud (blue) and high-cloud (red) coverage indices at Arica for 1200, 1800, and 2400 UTC. Total cloud cover (thick black), computed as the sum of the other two lines, aims at reproducing the results of Schulz et al. (2012) shown as thin black line with circles. See text for details.

Additionally, they provide trends for the 1971–96 period in stratocumulus daytime amounts, which average to +1.1% decade^{-1}, and in stratocumulus daytime heights, which average to +40 m decade^{-1}. The negative 1971–2009 cloud fraction trend and the positive 1971–96 cloud height trend conflict with our results presented in the previous sections.

Some of the discrepancies may be due to differences in the basic data used in each work. Three main differences are worth mentioning. First, while we use the basic cloud observations reported in section 3 of the SYNOP message, EW13 utilize the more aggregated and succinct cloud information present in section 1 of the SYNOP message (WMO 1995). Second, EW13 filter nighttime data for lunar illumination of clouds (Hahn et al. 1995), which we have not considered. Preliminary tests of the impact of lunar illumination on our results showed that for these stations it has little effect on averaged climatological properties. In terms of tendencies, while the seasonal pattern of cloud tendencies did not change, the filtered database showed somewhat smaller magnitudes in the tendencies (not shown). Finally, their results apply to averages of stations located in a 10° × 10° grid box, while our results are for individual stations. In particular, the values mentioned in the previous paragraph apply to a grid box located in northern Chile, which includes Iquique and Antofagasta stations but also four other stations located close to the Chilean coast more to the south.

The companion website of EW13 also provides access to their complete database so that a comparison with our data can be performed. Indeed, while up to 1996 both datasets agree well, in EW13's database the amount of available data for our three stations after 1996 drops to about 4% of that of the previous period. This drop is not present in our database, and the reason for its occurrence is unclear. However, it makes EW13's trends not representative of the full 1971–2009 period in this region. Moreover, EW13's database includes data for Iquique for periods 1971–75 and 1984–2009. The presence of data in the first period is suspicious considering that, as mentioned in section 2, the airport has operated at this site only since 1981. Finally, in terms of EW13's cloud height data, it must be pointed out that their basic data correspond to height categories coded in the synoptic reports. These codes have a coarse discretization in the range of stratocumulus heights in our region of interest. For example, codes 4, 5, and 6 are used for heights in the 300–600-, 600–1000-, and 1000–1500-m ranges, respectively. Although still not continuously distributed, Fig. 2c shows that our basic height data have more detailed estimates of cloud-base heights.

3) CLOUD FRACTION TENDENCIES OF QUINTANA AND BERRÍOS

Berríos (2008) and Quintana and Berríos (2007) performed preliminary analyses of the cloud data used in the present study. They reported long-term decreases in low-level cloud frequency, especially at Antofagasta. Again, these results appear to conflict with our findings in Fig. 5. In this case, the conflict is resolved by noticing that, although not explicitly said, their fractional cover averages were conditional to the existence of low-level clouds, which is different than the total averaged low-cloud

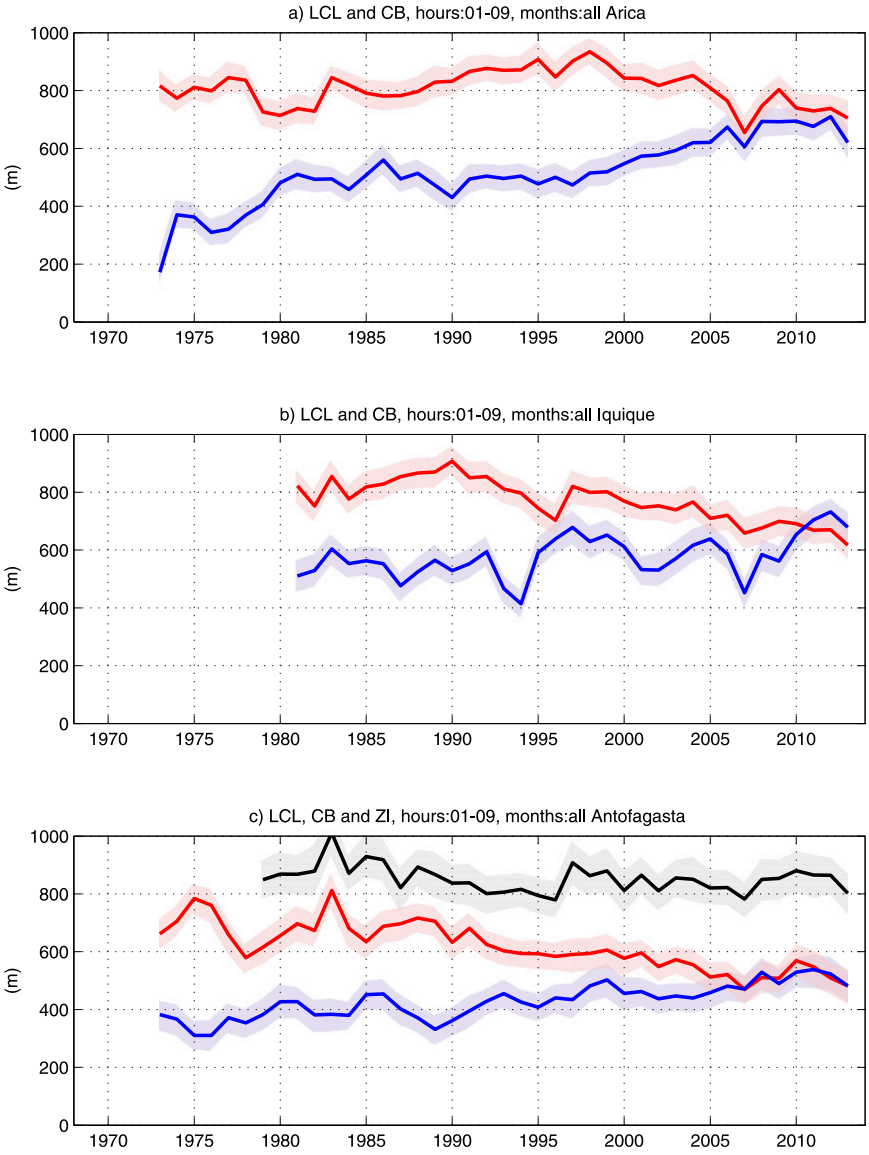

FIG. 12. Annual averages of cloud-base height (red) and surface LCL (blue) for (a) Arica, (b) Iquique, and (c) Antofagasta. Averages are computed for 0100–0900 UTC and nights that have mean low-cloud coverage greater than 7 oktas over the 0100–0900 UTC period. In (c) black line indicates the corresponding average of 1200 UTC subsidence ZI. Shading areas show estimated 95% confidence intervals for annual averages.

fraction computed in the present study, in which we consider a zero cloud fraction when no low-level clouds are reported. Thus, both results are consistent, as more frequent low-level clouds with smaller cloud coverages can produce a smaller conditional cloud fraction but a larger total cloud fraction average.

b. Cloud-base height and lifting condensation level tendencies

The two most conspicuous trends in variables described in section 3 are that of decreasing cloud-base heights and diminishing surface humidity. Figure 12 shows them together in the form of annual averages of CH and surface lifting condensation level (LCL) for cases with significant nighttime cloud coverage. The LCL was estimated by its approximate relationship to dewpoint depression, as described by Bohren and Albrecht (1998, p. 275). For most of the period, the mean LCL lies well below CH at the three sites, implying that in this coastal boundary layer (BL) there has not been a strong coupling between the surface and cloud layers. The opposing trends in CH and LCL, however, have led the two

variables to converge in recent years. This is especially noticeable at Antofagasta, where the annual means of both variables are almost identical since 2000, at the same time that the trends of both variables leveled off. The convergence of LCL and CH suggests that a stronger coupling of the BL has occurred in recent years. Indeed, Jones et al. (2011) and Zheng et al. (2011) report that the marine boundary layer near the coast of northern Chile appeared more coupled and well mixed than that offshore during the 2008 VAMOS Ocean–Cloud–Atmosphere–Land Study (VOCALS) regional experiment (Mechoso et al. 2014). However, without long-term observations of clouds offshore, it is not possible to ascertain whether the possible coastal coupling trend documented here has any counterpart offshore. On the other hand, the potential role of coastal circulation changes in the evolution of the degree of coupling of this coastal boundary layer is a possibility, but assessing it would require analysis of wind data and model results, which falls beyond the scope of the present work.

To better diagnose the degree of coupling of this coastal BL, we computed the interdaily correlation between LCL and CH for each station, at annual intervals (the same set of nights with large cloud cover used to construct Fig. 12 was used for these correlations). As expected for an uncoupled BL, the correlation between LCL and CH is small (less than 0.5) in almost all years and stations (not shown). The only exception is Antofagasta in which the correlation increases starting in 1990, reaching values between 0.5 and 0.70 after 2007. This may also be a sign of increased coupling of the BL at Antofagasta in recent years. In fact, using the last seven years of the record, the variance of CH explained by LCL is about 30%, while adding ZI as a factor increases the explained variance of CH up to about 50%. Considering that CH is visually estimated and ZI and LCL are completely independently measured, this cannot be considered a low variance fraction ($r \approx 0.7$).

At Antofagasta we have added in Fig. 12c the annual averages of ZI for the same set of days, derived from the 1200 UTC radiosondes launched routinely at this site. A slightly negative tendency for ZI is observed in Fig. 12c, consistent with the negative trend in ZI of $2\,\mathrm{m\,yr^{-1}}$ reported by Schulz et al. (2012). The smaller trend in ZI as compared to that of CH suggests that the coastal cloud layer may have been deepening in the last decades, from an average depth of about 200 m in the 1980s to about 300 m in the last decade. As in a cloud-topped boundary layer a main source of turbulence relates to radiative cloud-top cooling, the deeper cloud layer could be related to the stronger coupling of the BL suggested earlier. Another factor that could be favoring the deepening of clouds and the coupling of the boundary layer is the increase of the inversion strength capping the boundary layer as described by Seethala et al. (2015) and documented for the Antofagasta radiosonde database by Zamora (2010). Such strengthening would inhibit cloud-top entrainment and the subsequent evaporation of cloud water (Wood and Bretherton 2006).

c. *Humidity tendencies*

The drying of the near-surface air described previously poses two questions: 1) how to reconcile it with a cloud layer that may be becoming deeper and more frequent (at least in spring at Antofagasta; Fig. 5e) and 2) what its physical forcing could be. A possible answer to these questions could be that a stronger turbulent coupling of the BL makes the transport of humidity from the near surface toward the upper portion of the BL more efficient, thus drying the surface and presumably increasing the humidity at its top. The routine 1200 UTC radiosondes at Antofagasta allow, in principle, examination of this mechanism. Figure 13a shows the series of annual averages of the maximum relative humidity measured by these radiosondes in the 200–2000-m layer, in an attempt to characterize the humidity at the top of the coastal BL. In contrast with what was expected, a negative trend in humidity is suggested by Fig. 13a, especially in the 1986–2004 period. A clear jump is also noted in 2005, which is associated with a change in radiosonde equipment that occurred that year. Unfortunately, there is a lack of information regarding other possible changes in radiosonde equipment or procedures in other years, which makes the use of this radiosonde dataset to derive tendencies in humidity somewhat unreliable. Such problems in homogeneity of radiosonde humidity data for the computation of long-term trends have been extensively discussed by Dai et al. (2011).

Regarding the cause of the surface drying, another possibility is a reduction of the surface fluxes. Although there are no records of direct measurement of fluxes, another tendency suggested by the radiosonde dataset could be of interest here. Figure 13b shows the annual frequency of surface-based inversions in the 1200 UTC profiles (Muñoz et al. 2011). These inversions are typically shallow (median depth of 33 m) and weak (median temperature increment of 1 K), but they still may affect the turbulent surface exchange rates. Moreover, their apparent increase in frequency over the last three decades could point to a more stable atmospheric surface layer and a subsequent reduction in surface fluxes. This would be consistent with a coastal cooling driven by the ocean as suggested by Falvey and Garreaud (2009). Unfortunately, the lack of confidence in the homogeneity of this radiosonde dataset along the years pointed out earlier forces us to add a note of caution when interpreting the tendencies of Fig. 13b as well.

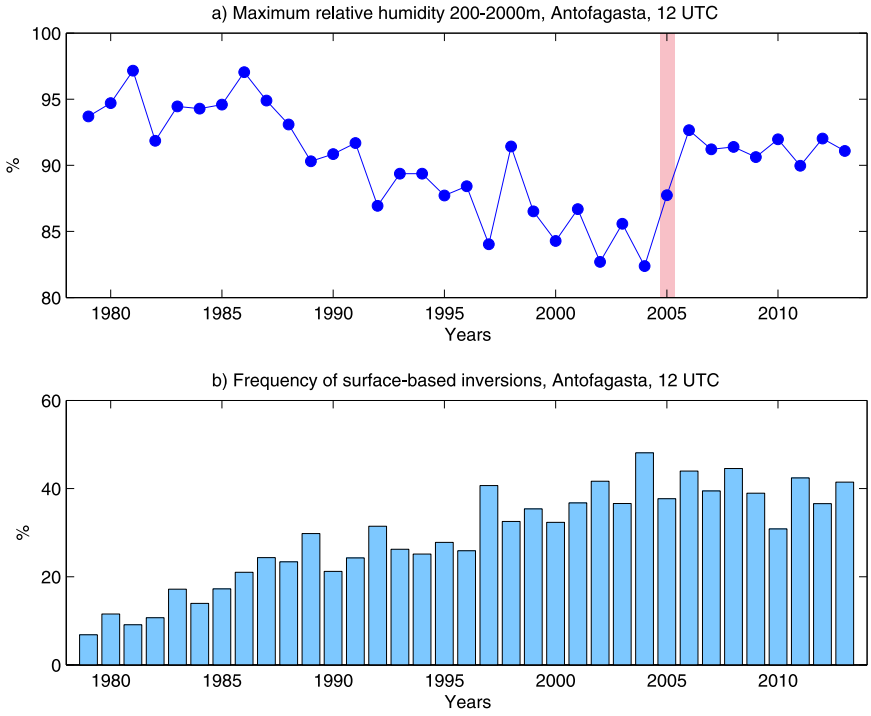

FIG. 13. (a) Annual averages of maximum relative humidity in the 200–2000-m layer derived from 1200 UTC radiosondes at Antofagasta. (b) Annual frequency of occurrence of surface-based inversions derived from 1200 UTC radiosondes at Antofagasta. A red shaded bar in (a) marks the occurrence of a documented instrumental change in radiosonde equipment.

6. Summary and concluding remarks

Based upon 33–45 years of hourly observations of cloud type, coverage, and heights at three sites along the northern Chilean coast (18.3°–23.4°S), we have documented here the climatology and trends of low-level coastal clouds at the eastern margin of the southeast Pacific. The diurnal cycle of cloud fraction shows a large amplitude at the three sites, especially in winter and spring, when average cloud fractions reach 7 oktas during some hours in the night while during daytime average values are between 2 and 3 oktas. The seasonal variation of low-level cloud coverage is characterized by maximum values in the austral winter and spring and minimum coverage in January–March (austral summer). The diurnal and seasonal variations of cloud-base heights are generally in opposite phase to that of cloud fraction: minimum values during the night and winter and maximum values in daytime and summer. Meridionally, nighttime cloud fraction and base heights are observed to increase from south to north, with the northernmost station, Arica, having nighttime clouds with the largest mean coverage and the longest persistence into morning hours.

Trends of cloud fraction show a seasonal modulation at the three sites, with increasing coverage in the spring (stronger in the southern stations) and a negative tendency in the fall (more marked in the northern stations). These trends are confirmed by independent measurements of sunshine hours at the sites, which show a consistent seasonal trend variation during daytime hours. Cloud-base heights, on the other hand, show generally negative trends at all stations. From south to north, these lowering trends begin around 1985, 1990, and 1995 at Antofagasta, Iquique, and Arica, respectively, ending around 2005 at Antofagasta.

The positive trends of cloud fractions during the cloudy season reported here conflict with previous studies that have described a negative tendency for cloud occurrence in this region. We attribute these discrepancies to differences in the datasets used (EW13; Schulz et al. 2012) or to methodological differences in the data analysis (Quintana and Berríos 2007). The lowering cloud-base height tendency is stronger than the lowering inversion base height at Antofagasta and appears consistent with the cloud fraction tendency, in the sense that a deeper and more fully covered cloud layer is becoming more frequent. The lowering cloud base is in principle also consistent with a cooling tendency for this coastal boundary layer as documented here and in previous studies (Falvey and Garreaud 2009; Vuille et al. 2015). However, we show here that this cooling has been accompanied by a drying of the near-surface air, a tendency that is difficult to

reconcile with more frequent low-level clouds. Assessing whether this intriguing result is caused by physical factors (e.g., increased aerosol load in the boundary layer or changes in the coastal circulation patterns) or by limitations of the data demands further analysis and more observations. In this respect, starting in August 2013 a continuously monitoring laser ceilometer is operating at the Antofagasta site, together with a total sky imager and an automatic weather station. It is expected that this new instrumentation will provide more detailed information on the dynamics of these coastal clouds and help answer some of the questions left open by the present work.

Acknowledgments. Partial funding by Project Fondecyt 1130111 is acknowledged. RG is partially supported by FONDAP Grant 15110009. Preliminary work on some of these topics by Patricia Berríos and Rosa Zamora is acknowledged. The authors thank three anonymous reviewers for their comments and suggestions. The authors express their appreciation to the numerous meteorological observers of the Dirección Meteorológica de Chile that have produced the long data records used in this work.

REFERENCES

Berríos, P., 2008: Stratocumulus in the coast of northern Chile: Variability and tendency (in Spanish). Undergraduate thesis, Dept. of Meteorology, University of Valparaíso, 118 pp.

Bohren, C. F., and B. A. Albrecht, 1998: *Atmospheric Thermodynamics*. Oxford University Press, 402 pp.

Bretherton, C., and Coauthors, 2004: The EPIC 2001 stratocumulus study. *Bull. Amer. Meteor. Soc.*, **85**, 967–977, doi:10.1175/BAMS-85-7-967.

Dai, A., J. Wang, P. W. Thorne, D. E. Parker, L. Haimberger, and X. L. Wang, 2011: A new approach to homogenize daily radiosonde humidity data. *J. Climate*, **24**, 965–991, doi:10.1175/2010JCLI3816.1.

Eastman, R., and S. G. Warren, 2013: A 39-yr survey of cloud changes from land stations worldwide 1971–2009: Long-term trends, relation to aerosols, and expansion of the tropical belt. *J. Climate*, **26**, 1286–1303, doi:10.1175/JCLI-D-12-00280.1.

——, and ——, 2014: Diurnal cycles of cumulus, cumulonimbus, stratus, stratocumulus, and fog from surface observations over land and ocean. *J. Climate*, **27**, 2386–2404, doi:10.1175/JCLI-D-13-00352.1.

Falvey, M., and R. Garreaud, 2009: Regional cooling in a warming world: Recent temperature trends in the southeast Pacific and along the west coast of subtropical South America (1979–2006). *J. Geophys. Res.*, **114**, D04102, doi:10.1029/2008JD010519.

Garreaud, R., 2011: The climate of northern Chile: Mean state, variability and trends. *Rev. Mex. Astron. Astrofis.*, **41**, 5–11.

Hahn, C. J., S. G. Warren, and J. London, 1995: The effect of moonlight on observation of cloud cover at night, and application to cloud climatology. *J. Climate*, **8**, 1429–1446, doi:10.1175/1520-0442(1995)008<1429:TEOMOO>2.0.CO;2.

Jones, C. R., C. S. Bretherton, and D. Leon, 2011: Coupled vs. decoupled boundary layers in VOCALS-REx. *Atmos. Chem. Phys.*, **11**, 7143–7153, doi:10.5194/acp-11-7143-2011.

Klein, S., and D. Hartmann, 1993: The seasonal cycle of low stratiform clouds. *J. Climate*, **6**, 1587–1606, doi:10.1175/1520-0442(1993)006<1587:TSCOLS>2.0.CO;2.

Mechoso, C. R., and Coauthors, 2014: Ocean–cloud–atmosphere–land interactions in the southeastern Pacific: The VOCALS program. *Bull. Amer. Meteor. Soc.*, **95**, 357–375, doi:10.1175/BAMS-D-11-00246.1.

Muñoz, R. C., R. Zamora, and J. Rutllant, 2011: The coastal boundary layer at the eastern margin of the southeast Pacific (23.4°S, 70.4°W): Cloudiness-conditioned climatology. *J. Climate*, **24**, 1013–1033, doi:10.1175/2010JCLI3714.1.

Quintana, J., and P. Berríos, 2007: Study of the coastal low cloud in the northern coast of Chile: Variability and tendency. *Proc. Fourth Int. Conf. on Fog, Fog Collection and Dew*, La Serena, Chile, FogQuest, 189–192.

Rondanelli, R., A. Molina, and M. Falvey, 2015: The Atacama surface solar maximum. *Bull. Amer. Meteor. Soc.*, **96**, 405–418, doi:10.1175/BAMS-D-13-00175.1.

Schulz, N., J. P. Boisier, and P. Aceituno, 2012: Climate change along the coast of northern Chile. *Int. J. Climatol.*, **32**, 1803–1814, doi:10.1002/joc.2395.

Seethala, C., J. R. Norris, and T. A. Myers, 2015: How has subtropical stratocumulus and associated meteorology changed since the 1980s? *J. Climate*, **28**, 8396–8410, doi:10.1175/JCLI-D-15-0120.1.

Sydeman, W. J., M. García-Reyes, D. S. Schoeman, R. R. Rykaczewski, S. A. Thompson, B. A. Black, and S. J. Bograd, 2014: Climate change and wind intensification in coastal upwelling ecosystems. *Science*, **345**, 77–80, doi:10.1126/science.1251635.

Trenberth, K. E., and J. T. Fasullo, 2013: An apparent hiatus in global warming? *Earth's Future*, **1**, 19–32, doi:10.1002/2013EF000165.

Varela, R., I. Álvarez, F. Santos, M. de Castro, and M. Gómez-Gesteira, 2015: Has upwelling strengthened along worldwide coasts over 1982–2010? *Sci. Rep.*, **5**, 10016, doi:10.1038/srep10016.

Vuille, M., E. Franquist, R. Garreaud, W. S. Lavado Casimiro, and B. Cáceres, 2015: Impact of the global warming hiatus on Andean temperature. *J. Geophys. Res. Atmos.*, **120**, 3745–3757, doi:10.1002/2015JD023126.

Warren, S. G., R. Eastman, and C. J. Hahn, 2007: A survey of changes in cloud cover and cloud types over land from surface observations, 1971–96. *J. Climate*, **20**, 717–738, doi:10.1175/JCLI4031.1.

Wilks, D. S., 2005: *Statistical Methods in the Atmospheric Sciences*. 2nd ed. Academic Press, 648 pp.

Williams, A. P., R. E. Schwartz, S. Iacobellis, R. Seager, B. I. Cook, C. J. Still, G. Husak, and J. Michaelsen, 2015: Urbanization causes increased cloud base height and decreased fog in coastal Southern California. *Geophys. Res. Lett.*, **42**, 1527–1536, doi:10.1002/2015GL063266.

WMO, 1995: Manual on codes. WMO Rep. 306, 492 pp.

Wood, R., 2012: Stratocumulus clouds. *Mon. Wea. Rev.*, **140**, 2373–2423, doi:10.1175/MWR-D-11-00121.1.

——, and C. S. Bretherton, 2006: On the relationship between stratiform low cloud cover and lower-stratospheric stability. *J. Climate*, **19**, 6425–6432, doi:10.1175/JCLI3988.1.

Zamora, R., 2010: Observational characterization of the marine boundary layer in Antofagasta (in Spanish). M.S. thesis, Dept. of Geophysics, University of Chile, 122 pp.

Zheng, X., and Coauthors, 2011: Observations of the boundary layer, cloud, and aerosol variability in the southeast Pacific near-coastal marine stratocumulus during VOCALS-REx. *Atmos. Chem. Phys.*, **11**, 9943–9959, doi:10.5194/acp-11-9943-2011.